A BIOMECHANICAL ASSESSMENT OF PERI-IMPLANT BONE TISSUE: EFFECT OF MATERIAL MODEL HOMOGENEITY ON STRAIN DISTRIBUTION IN MANDIBLE

Thomková B.*, Marcián P.**, Borák L.***

*Bc. Barbora Thomková.: Institute of Solid Mechanics, Mechatronics and Biomechanics, Faculty of Mechanical Engineering, Brno University of Technology, Technická 2896/2, 616 69 Brno, Czech Republic; CZ
**Ing. Petr Marcián, PhD.: Institute of Solid Mechanics, Mechatronics and Biomechanics, Faculty of Mechanical Engineering, Brno University of Technology, Technická 2896/2, 616 69 Brno, Czech Republic; CZ
***Ing. Libor Borák, PhD.: L.K. Engineering, s.r.o., Vídeňská 55, 639 00 Brno, Czech Republic; CZ

1. INTRODUCTION

Insertion of the dental implant is nowadays a routine operation. Implants are mostly inserted in the healed alveolar bone of the mandible or the maxilla and their performances are highly efficient, reliable and with low post-operative complications. This is mainly because of a phenomenon called osseointegration which takes advantage of implant surface (commonly titanium alloy) and enables its firm integration with newly grown bone. Despite the positive role of the osseointegration, there is still a possibility of implant failure due to unfavorable mechanical loading.

The aim of this study is to compare mechanical performances of bone-implant interaction when different material representations (homogeneous and non-homogeneous material model of bone tissue) are used in the computational modelling.

2. METHODS

For the computational modeling purposes, the same CT dataset was used for all investigated cases. The human mandible was scanned on CT (Philips) with voxel size 0.49 mm x 0.49 mm x 0.45 mm.

2.1 GEOMETRY MODEL

The CT images were segmented using manual and automatic segmentation in STL Model Creator software (Marcián et al. 2011) to obtain 3D geometry model of the human mandible. Manual segmentation was used to create geometry model of cortical bone with variable thickness. Geometry model of Brånemark dental implant (Brånemark® System Mk III Groovy (NP Ø 3.3 mm, 11.5 mm)) was made in SolidWorks 2012 (Dassault Systèmes, France). The dental implant was inserted in healed alveolar bone in the molar region (see Fig.1).

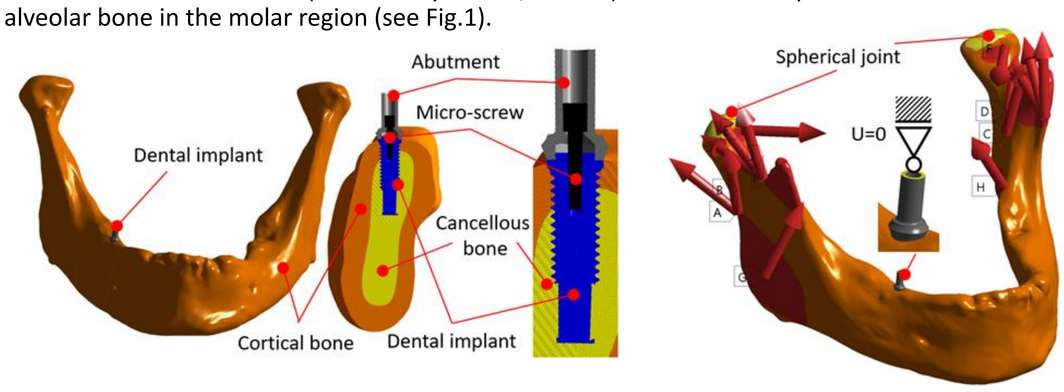

Fig. 1 Geometry model: position of Brånemark dental implant inserted in the mandible.

2.2 MATERIAL MODEL

Dental implant and bone tissues were modelled assuming material linearity, isotropy, homogeneity (with one exception discussed below) and elasticity, i.e. using two elastic constants; Young's modulus (E) and Poisson's ratio (μ). Material model of dental implant and cortical bone were modeled based on the findings of (Kayabasi et al. 2006) (E=110000 MPa and μ=0.34) and (Menicucci et al. 2002) (E=13700 MPa and μ=0.3), respectively.

Three variants of cancellous bone material models were analyzed. The first two variants were analyzed assuming homogeneous distribution of Young's modulus in the whole cancellous bone representation (with two different moduli for each variant). The third variant was based on a non-homogeneous material distribution which complied with grey values of the CT images (Lin et al. 2009, Borák et al. 2017) (see Fig. 2). The same Poisson's ratio (μ=0.3) was used for all variants of cancellous bone. The modulus for the first cancellous bone model variant has been chosen based on literature (Menicucci et al. 2002) E=1370 MPa (labelled as E_{1370}). The modulus for the second variant has been calculated from the average Hounsfield unit value (HU=438.9) obtained out of all bone-related pixels of 30 CT images that corresponded to the modelled geometry. The calculation was performed using Eq. (1) (Cheng et al. 2019) and Eq. (2) (O'Mahony et al. 2000):

$$\rho = 0.114 + 0.000916 \cdot \mathrm{HU}\ [\mathrm{g/cm^3}] \quad (1)$$

$$E = 2349 \cdot \rho^{2.15}\ [\mathrm{MPa}] \quad (2)$$

where ρ is bone density. From these equations, E=566 MPa (labelled as E_{566}) was obtained.

The third material model was generated using software CTPixelMapper (using Eq. (1) and Eq. (2)) that mapped CT-image-pixel-specific E into the FE model (Borák et al. 2017) (labelled as E_{CT}).

2.3 LOAD AND BOUNDARY CONDITIONS

To simulate chewing, it is necessary to consider constraints in the area of condyles and also in the area of application of biting forces (see Fig. 1). Spherical joints were used in the condylar area avoiding displacement in all directions. A remote displacement condition was also applied in axial direction of the implant to avoid axial displacement. Mandible was loaded by forces applied in locations of muscle attachments and in directions of those muscles (Korioth et al. 1996), (see Fig. 1).

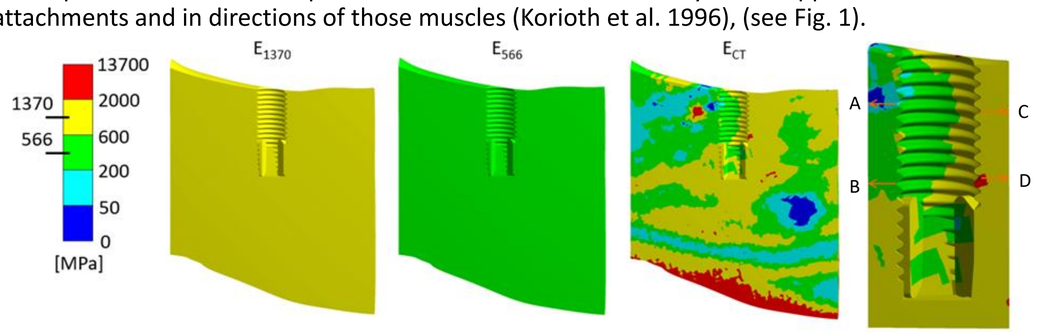

Fig. 2 Three variants of material model of cancellous bone tissue, highlighted paths A-D.

ACKNOWLEDGEMENT
The research was supported by the Czech Science Foundation by grant No. 16-08944S. This work was supported by grant specific research FSI-S-20-6175.

2.4 FE MESH

All components were assembled using a FE simulation tool of ANSYS® Academic Research Mechanical, Release 19.2 (Swanson Analysis, Inc. Houston, PA, USA). Each model was meshed by SOLID187 elements which are of a quadratic tetrahedral element type. The default element size was used in majority of FE mesh except for the very peri-implant region. This region (including the implant) was meshed by SOLID187 and the general size of element was 0.45 mm. This minimum size was chosen based on a previous study (Borák et al. 2017). The implant threads as well as the bony faces which were in contact with the implant were meshed by elements sized 0.04 mm. The whole model consisted of 3055321 nodes. The mechanical interaction between the implant and the bone was modeled by contact elements CONTA174 and TARGE170. For the interacting components (bone+implant), "always bonded" contact type was used with the multipoint constraint contact formulation. This contact option mimicked the assumed perfect osseointegration

3. RESULTS AND DISCUSSION

Strain intensity distribution within peri-implant regions in cancellous bone tissue of all variants are shown in Fig. 3. The color ranges were adjusted to correspond with strain intensity intervals suggested by Mechanostat hypothesis (Lin et al. 2009). The cancellous bone was strained the most in the region of implant apex regardless of the material model variant. The highest strain intensity was observed in E_{566} variant.

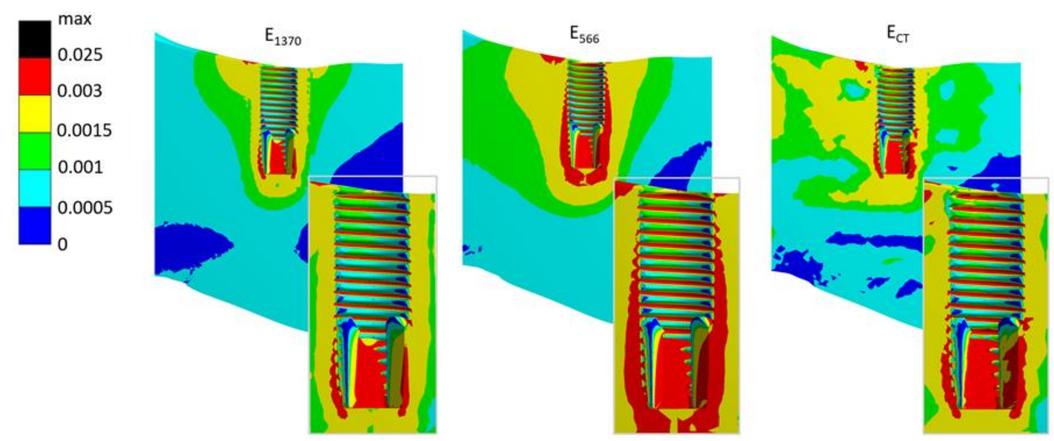

Fig. 3 Strain intensity in cancellous bone .

Four paths through the peri-implant bone were assumed for the purpose of the quantitative analysis (see Fig. 2). Strain intensity along these paths are presented in Fig. 4. Graphs show that strains decrease with increasing distance from the implant surface with a significant threshold being at approx. 0.1 mm from the implant (observed in all variants). Up to the 0.1 mm distance, the bone is pathologically overloaded exceeding Mechanostat-based strain intensity threshold of 0.003. Beyond this distance, the strains in bone are below the value of 0.003 and, therefore, comply with the physiological condition. On paths A and B on one side of the implant, the bone density varies between 0.15-0.22 g/cm^3 and 0.43-0.52 g/cm^3, respectively. On the other side on paths C and D, the bone density is almost 2-times higher ranging between 0.73-0.79 g/cm^3 and 0.77-0.94 g/cm^3, respectively. As the elastic properties of the bone and hence the strain results depend on the bone density distribution within the region of interest, it is appropriate to use E_{CT} variant if the existing density variability is not to be omitted. The correspondence of paths C and D results based on E_{1370} and E_{CT} models is purely coincidental (actual bone densities on those paths are close to the average value that was used for calculating E_{1370}).

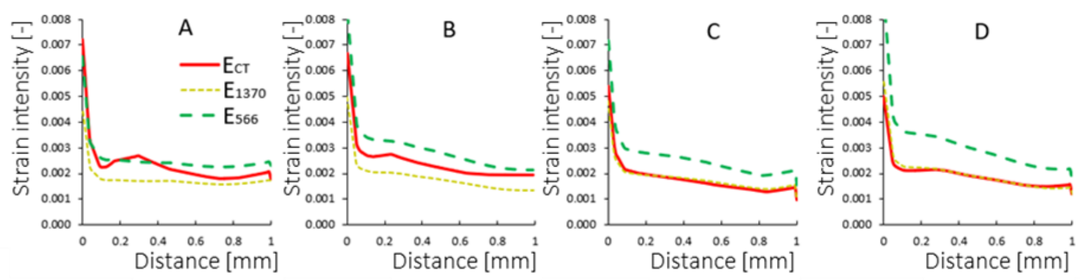

Fig. 4 Strain intensity along paths A, B, C and D.

4. CONCLUSION

This paper deals with an analysis of mechanically loaded peri-implant bone using computational modeling. The character of strains in the peri-implant region (up to 0.1 mm from the implant) is influenced dominantly by the geometry of the selected dental implant than by the used material model variant. Beyond a threshold of 0.1 mm, local bone density plays an important role that should be addressed by a proper selection of material model variant. To perform more credible analysis of local strains in the peri-implant region, it is preferable to adopt material model based on CT images.

REFERENCES

Borák, L., Marcián, P. (2017) Inhomogeneous Material Properties Assignment to Finite Element Models of Bone: A Sensitivity Study. In Engineering Mechanics 2017, p. 190-193.
Cheng, K., Liu, Y., Wang, J., Jun, J., Jiang, X., Wang, R., Baur, Z. (2019) Biomechanical behavior of mandibles reconstructed with fibular grafts at different vertical positions using finite element method. Journal of Plastic, Reconstructive & Aesthetic Surgery, 72 , pp. 281-289.
Kayabaşı, O., Yüzbasıoğlu, E., Erzincanlı, F. (2006) Static, dynamic and fatigue behaviors of dental implant using finite element method. Advances in Engineering Software, 37, pp.649-658.
Korioth, T.W.P. and Hannam, A.G. (1996) Deformation of the Human Mandible During Simulated Tooth Clenching, Journal of Dental Research, 73, pp. 56-66.
Marcián, P., Konečný, O., Borák, L., Valášek, J., Řehák, K., Krpalek, D., Florian, Z. (2011) On the Level of Computational Models in Biomechanics Depending on Gained Data from Ct/Mri and Micro- Ct, MENDEL 2011 - 17th International Conference on Soft Computing. 1, pp. 255-267.
Menicucci, G., Mossolov, A., Mozzati, M., Lorenzetti, M., Preti, G. (2002) Tooth-implant connection: some biomechanical aspects based on finite element analyses. Clinical Oral Implants Research, 13, pp. 334-341.
O'Mahony, A., Williams, J., Katz, J.,Spencer, P. (2000) Anisotropic elastic properties of cancellous bone from a human edentulous mandible. Clinical Oral Implants Research, 11, pp. 415-421.

BRNO UNIVERSITY OF TECHNOLOGY FACULTY OF MECHANICAL ENGINEERING